Paddy and Water Environment (2022) 20:395–412
https://doi.org/10.1007/s10333-022-00901-x

ARTICLE

Crop type detection using an object-based classification method and multi-temporal Landsat satellite images

Neamat Karimi[1] · Sara Sheshangosht[1] · Mortaza Eftekhari[1]

Received: 7 August 2021 / Revised: 11 April 2022 / Accepted: 12 April 2022 / Published online: 14 May 2022

Abstract

Crop type detection is of great importance in water resource allocation and planning mostly in arid and semi-arid regions of Iran. Landsat-OLI 16-day inter-annual images are invaluable sources obviating crop monitoring into issues of crop types detection, crop yield prediction, and crop pattern studies. Although many classification methods such as decision tree (DT), support vector machine (SVM), and maximum likelihood (ML) were implied for crop type mapping, recent researches often use an object-based classification approach. In this study, an object-based image analysis (OBIA) classifier based on rule-based decision tree (RBDT) and object-based nearest neighbor (OBNN) used to delineate five common crop types (includes Wheat and Barley together in one class, rice, multiple crop (MC), Alfalfa and Spring crops) in Isfahan city and nearby areas. The classification was applied in five scenarios using different vegetation indexes including normalized difference vegetation index (NDVI), normalized difference water index (NDWI), green normalized difference vegetation index GNDVI and their combination. All scenarios property and accuracy assessed both with by class separation distance matrix and confusion matrix. The overall accuracy of classification with using only one vegetation index was lower than other scenarios. It was the lowest for GNDVI rating 37% whereas combination of Indexes resulted better accuracy. In final map with combination of NDVI, GNDVI and NDWI, overall accuracy and kappa achieved to 88% and 0/83 successively. Comparing individual accuracy of different crops showed that MC crops with 66% has the lowest accuracy and Wheat-Barely crops with 94.8% individual accuracy has the Maximum accuracy. Other crop types accuracy alters between 66 and 94.8%.

Keywords Crop type · Object based image analysis · Segmentation · NDVI · NDWI

Introduction

Crop type detection is a critical and important parameter in food security, land use monitoring, and water resource management affecting climate change and biodiversity. Knowledge of crop type and distribution across landscapes is essential for agricultural lands management and development in a sustainable manner (Schreier et al., 2020). Water consumption of various crop types is a challenging issue in water resource management addressed by croplands mapping and monitoring. It is more highlighted in arid and semi-arid areas like the central part of Iran, facing with lots of water allocation challenges to agricultural activates (Asgarian et al. 2016). Also, crop type information obviates croplands water resources future planning and management considering environmental factors like climate changes (Immitzer et al. 2016). Accordingly, an accurate crop type classification has become one of the main objectives in the field of agriculture and related domains.

While, manual and field approaches for mapping crop types (e.g., interviews with farmers and local communities) are time consuming and laborious, remote sensing methods are rich, reliable data sources for monitoring the earth surface, crop types, and temporal behaviors of croplands in growing seasons (Castillejo-González et al. 2009; Peña-Barragán et al. 2011; Manakos and Lavender 2014). Moderate spatial resolution satellite images (e.g., MODIS, Sentinel and Landsat images) are widely used to map Land Use Land Cover (LULC) and their changes over time (Huang

✉ Neamat Karimi
n.karimi@wri.ac.ir; nehmatkarimi@gmail.com

Sara Sheshangosht
sara_shesh@yahoo.com

Mortaza Eftekhari
mortazaeftekhari@gmail.com

[1] Department of Water Resources Study and Research, Water Research Institute, Tehran, Iran

2007; Ulaby 1982; Sencan 2004). Besides, many vegetation indices synergic with satellite images have been developed to estimate the type of crop (Pani et al., 2020; Gerstmann et al., 2018). For example, global Cropland maps were produced using MODIS 250-m and 500-m NDVI yearly and seasonally time series (Wang et al. 2014a, b) and on some occasions has focused on rain-fed crops (global map of rain fed cropland areas (GMRCA)) or irrigated croplands (global irrigated area map (GIAM)) (Thenkabail et al. 2009). Understanding the phenology of croplands obviates crop type detection and reduce time series images for crop type mapping. Phenology map of OWA, the United States of America (USA) produced by using combination of Landsat 5, 7, 8, and MODIS data (Gao et al., 2017).although,, MODIS time series is a common source in croplands studies, due to the coarse spatial resolution of 250-m it is suitable for large open fields ((Lebourgeois et al., 2017)}and surges the uncertainties of the results especially in mixture crop types like Africa (Vancutsem et al. 2012). Therefore, using high resolution satellite images like Landsat, ASTER, Sentinel, and very high spatial resolution satellite images like RapidEye, GeoEye, and IRS-P5 has been considered as a viable source in the last decade (Gerstmann et al., 2018). Among medium spatial resolution satellite images, Landsat 16-day long-term and its cost-effective archive has been known as an invaluable data source used frequently to extract crop type classification (Khan et al., 2020; Chen et al., 2020). However, using Landsat archive images has some limitation, cloud cover in cold seasons, 16-day revisit time and 30 m resolution which is not suitable for smallholder croplands. Therefore, recently, using Sentinel-1 and Sentinel-2 images has become more popular for crop type mapping (Chen et al., 2020). For example, Sentinel-2 and RapidEye images used to produce crop type maps of Austria and Germany (Immitzer et al. 2016; Gerstmann et al. 2016).while, Landsat images vegetation indices time series is using for national crop land classification National Agricultural Statistics Service (NASS) of the United States Department of Agriculture produced seven states, Arkansas, Illinois, Indiana, Iowa, Mississippi, New Mexico, and North Dakota, cropland map using Landsat-5 and Landsat-7 images in 2001 with other agricultural Agencies cooperation (Craig 2010). Integration of Landsat, ASTER, and MODIS images from April to August utilized to produce the Land cover map and crop type inventory of Tiffani watershed (Brooks et al. 2006). Additional to time series of (Landsat-Sentinel) images, different vegetation indices time-series. Normalized difference Vegetation Index (NDVI) and Normalized difference Water Index (NDWI) have being used in crop type detection. NDVI time series is the principle index using for vegetation dynamic/phenology monitoring in crop type studies and NDWI usually utilize for determination of well-watered crops (Ferrant et al., 2017) (Gerstmann, 2018). Time series of NDVI, and NDWI of Landsat-8 images used with decision tree classification method in R software to extract irrigated cropland pattern and fallow-lands rotation in six block in Gash Delta of Sudan (Fujihara, 2020). Although Landsat spatial resolution is better than MODIS images, the 16-day revisit time of images (which might increase to 32 or more according to the cloud covers in each region) is a hindrance in the detection of some crops growing promptly or harvesting in small growing periods (e.g., vegetables, cucumber) (Hilker et al. 2009). So, NDVI times series of MODIS images are using as an assistant dataset to detect the crops calendar/phenology and for crop types with short growing seasons, daily NDVI (NDVI of MODIS images) offers better results (De Castro et al. 2018).

Crop type extraction accuracy using remote sensing data depends on some contributing factors: (1) spatial and temporal resolution of satellite images, (2) crop types phenology difference (Robson et al. 2012), (3) spectral similarity of each crop type with other land covers, (4) crops variation in each region (Fritz et al. 2011) and (5) methodology used for crop type classification. The factor (2),(3) and (4) are highly depend on the crops phenology and the physical parameters of studying area and also has less dependency to remote sensing datasets and classification methods. On the other hand, satellite image, their temporal and spatial resolution and more importantly, the method used for classification have a significant effect on the accuracy of the crop type mapping results. All image classification methods are categorized into pixel-based and object-based classification approaches. In pixel-based image classification methods, the rate of misclassification over the agricultural areas is high due to the several reasons: A) similar spectral characteristics of some agricultural classes, B) spectral variability of the canopy reflectance and the bare soil background within an agricultural field and, C) the presence of mixed pixels located at the boundary between classes (De Wit and Clevers, 2004). Also, small cropland pixels may be considered as noise in post-processing step and they might eliminate. Consequently, evaluation of the accurate area of each cropland might be erroneous. To address these problems, OBIA has become more popular in remote sensing analysis in which the whole shape of each land is preserved by assigning a correct class to the land. OBIA classifier creates homogenous cropland parcels based on spectral and spatial similarity of image objects (crop fields).In recent decades by the advancement of geomatics technologies in remote sensing and GIS and the availability of medium to high spatial resolution images like Landsat-OLI, Sentinel-1 and 2, Spot, RapidEye, and Worldview, object-based image classification approaches are taken into action in crop discrimination (Torbick et al., 2017; Kussul et al., 2017). Object-based image classification methods promised better crop detection studies in contrast with pixel-based classification (Zaki et al., 2020).

OBIA classification includes two basic steps, segmentation, and classification. 1) in the segmentation process the user can control the size and shape of the segments (croplands) as a desirable scale and 2) classification conducts by using textural, morphological, and shape indicators and also the spectral indicators for each segments, (crop lands) in this study. In this case, each cropland not only extracts based on its spectral factors but also based on its' spatial factors like rectangular fitness, compactness, similarity and texture and finally OBIA classifier extracts croplands similar to human vision. OBIA method used for crop type classification of Southwest Missouri based on combination of NDVI time series of Landsat and MODIS images (Li et al., 2015). Also, Crop type map of Ukraine derived using neural network OBIA based on combination of Landsat-OLI and sentinel-1 images and it upgraded to an operational system (Sen2-Agri) by which a thematic crop map produce in a demanded resolution based on the user defined data for five major crop types {Kussul, 2016 #18}{Lukas Blickensdörfer, 2022 #63}.. OBIA DT based on Landsat (ETM^+ and TM) images time series and field observation data utilized to extract sugarcane lands of Brazil admittedly separated from soybean and other land covers in Missouri (Li et al. 2015; Vieira et al. 2012). Time series of different vegetation indices besides the multi spectral images play a principle role for crop types phenology and signature detection and in the many of crop mapping studies, the focus is on the variation of theses indices (e.g. NDVI, EVI, and NDWI). Different Land cover classification methods assessment utilized NDVI and NDWI indices of Sentinel-2 imagery with suite observation and European crop parcel maps with combination of Sentinel-2 and sentinel-1 with a large amount of situ observation derived with random forest classifier (Weigand et al. 2020). Landsat OLI time series and enhanced vegetation index (EVI) based on random forest and data mining decision tree techniques were the main satellite data to crop mapping of Cerrado, Brazil (Do Bendini et al. 2016) Crop types map in two European cities (in Italy and Romania) and one American city (in California) classified from Sentinel-2 (NDVI) time series both with OBIA and pixel-based methods. They showed that the OBIA methods results are more accurate and feasible than pixel based methods. (Belgiu and Csillik, 2018). Multi temporal SPOT5 images in in Baishan with ruleset OBIA method conducted for crop type mapping and it showed higher accuracy and less time consuming for crop type mapping (Dongping Ming et al., 2016). OBIA throughout segmentation offers a feasible method reducing spectral differences within various classes and salt and paper effects on thematic maps, increase classification accuracy with incorporating texture, object related information(Peña-Barragán et al., 2011).

Accurate and timely cropland maps of agricultural lands of Iran are essential for water resource managing, optimal water allocation and updating agriculture databases regarding to developments and plans. Therefore, the development of an operational method with appropriate accuracy to determine the crop types is very important and necessary for Iranian agricultural lands. This study investigates the performance of using multi-temporal Landsat 8 imagery with different vegetation indices for crop differentiation based on object-based classification. The main goals of this study are to provide: 1) Crop type detection (includes wheat and barley, rice, alfalfa, multi-cops and spring crops with an OBIA classification in Isfahan and nearby areas of the Zayandeh-Rud river using multi-temporal Landsat satellite images, 2) evaluating the potential of different multi-temporal vegetation indexes (NDVI, NDWI, and GNDVI) in crop type detection. The results are interpreted in the context of finding an operational solution for monitoring crop types over extensive areas.

Study area

The study area is located in the south of Isfahan Province at the central part of the Gavkhoni basin, a major basin in the central plateau of Iran, vitally important to state its environmental impacts on crop yield and water resources. Its area is about 8800 km^2 and geographically located between 31.7369° N to 33.2947° N latitude and 50.8755° E to 51.9817° E Longitude based on Datum of WGS84 as shown in Fig. 1. Also, this region contains the central part of the Zayandeh-Rud River and Nekoo-Abad dam in the southern part of Isfahan which terminates to Gavkhoni lagoon. Also, it contains agricultural suburbs of Isfahan, Mubarak-e, Borkhar, and Najaf-Abad cities, historically been reputed for rice, wheat and barley, and orchard products. The study area is located in the lush plain of the Zayanderud River at the foothills of the Zagros mountain range. The annual precipitation varies from 1500 mm in the west to 50 mm in the east of the basin. Also, the mean annual temperature of this area is about 17.5 °C with the mean relative humidity of about 42%. The Zayandeh-Rud River, with an average natural flow of 1400 million cubic meters (mcm) per year, including 650 mcm of natural flow and 750 mcm of inter-basin transferred flow, starts in the Zagros Mountains in the west of the basin and ends in the Gav-Khuni Marsh in the east of the basin. Currently, more than 73% of the basin's available water resources are used for agriculture (Fig. 2).

Recently, the industrial expansion of capital cities like Isfahan made some Land use changes in the city and suburbs. Therefore, the traditional crops are substituted with industrial crops such as MC, spring crops, and alfalfa with higher economic advantages to farmers as a contributing factor. Cropland investigation in this area by Asgarian and Akbari are good examples showing the significance of

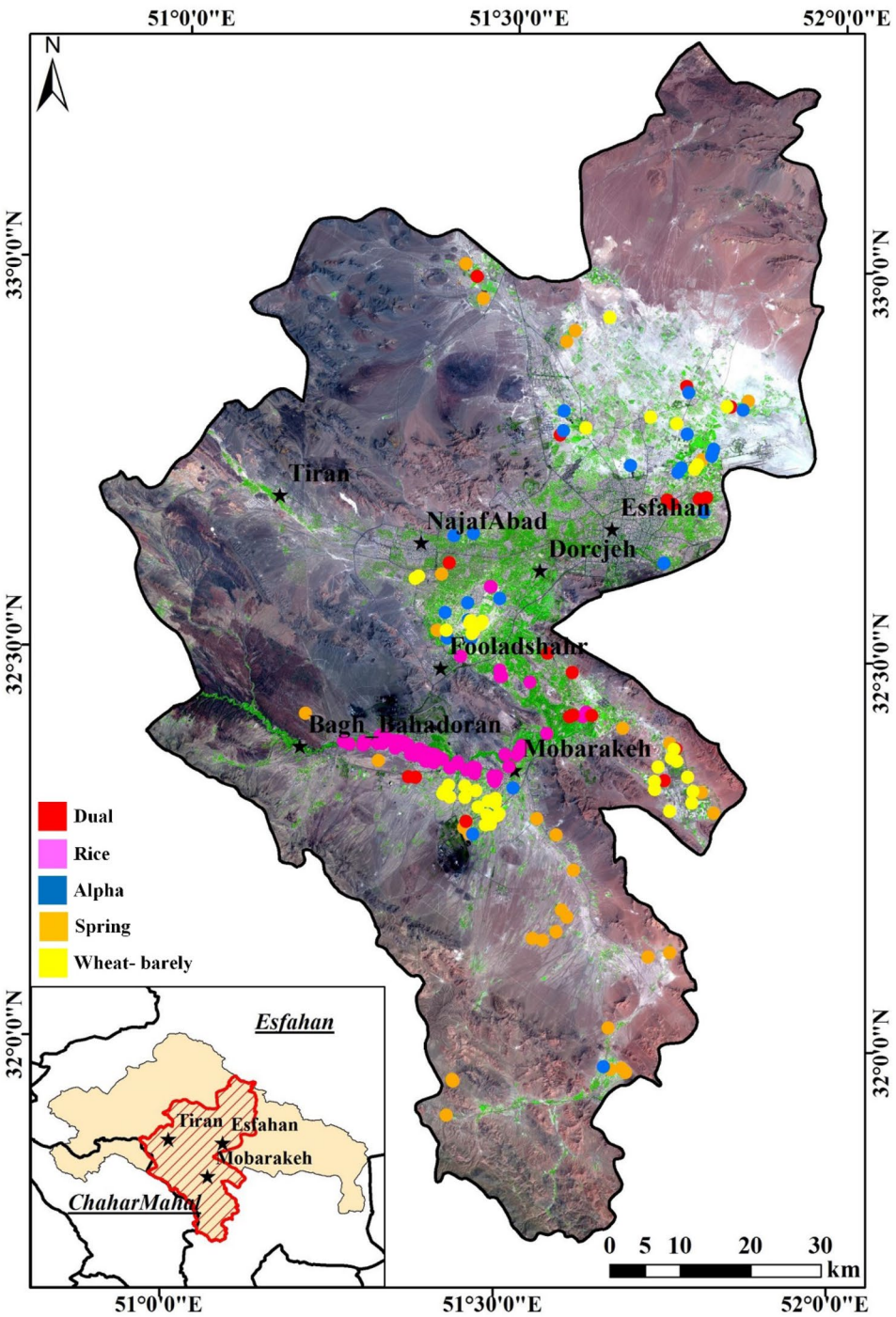

Fig. 1 Location map of the study area and the spatial distribution of field data

cropland detection and change. They extracted alfalfa and rice in some parts of the Zayandeh-Rud basin in the recent decade. On the other hand, agriculture and drinking water needs of this area are mainly dependent on the Zayandeh-Rud River. Recent researches have shown that extra water extractions for irrigation systems and domestic uses made the river dye out to Gavkhoni lagoon while affecting water quality and soli salinity, restricted agricultural activates, and reduced agricultural land size. Therefore, crop type detection due to land use and water management is more highlighted in this area (Molle and Wester 2009; Asgarian et al. 2016). Although, the new agricultural plan is not recommended in order to water resources shortage and vulnerable soil condition, many crop types changes have happened recently which urgently enhance crop type delineation. Akbari in 2006 prepared a crop map in some parts of the Zayandeh-Rud basin using a single-date Landsat-7 image with a maximum likelihood classifier. Later in 2016, similar research has done

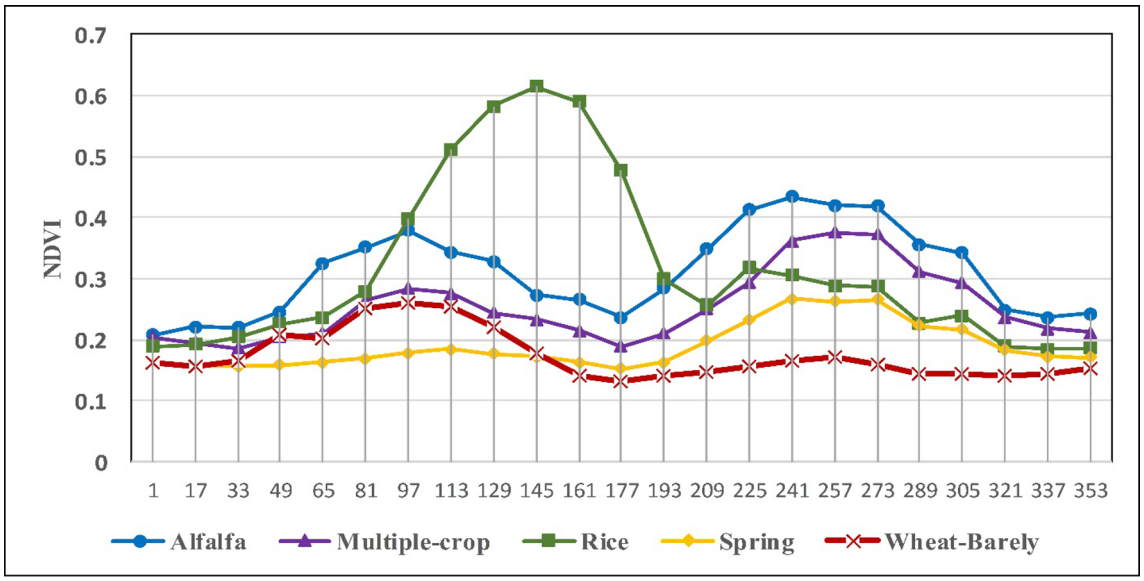

	Jan 1	Jan 17	Feb 33	Feb 49	Mar 65	Mar 81	Ap 97	Ap 113	May 129	May 145	June 161	June 177	July 193	July 209	Aug 225	Aug 241	Sep 257	Sep 273	oct 289	oct 305	Nov. 321	Dec. 337	Dec. 353
Alfaalfa																							
Multiple crop																							
Rice																							
Spring crop																							
Wheat-Barley																							
All_crops																							

Fig. 2 The graph of average NDVI time series of 5 crop type by MODIS Images. The colored boxes in the bottom table of Fig. 2 show the date of growing seasons of each crop type. The uncolored boxes belong to sewing or harvesting dates

in a small part of the studying area, NajafAbad, using five Landsat images by Asgarian (Asgarian et al. 2016).

Materials

Dataset

Multi-temporal MODIS NDVI data for generating crops calendar

Multi temporal of MOD13Q1 products of MODIS images containing NDVI data in 2016 used at spatial resolution of 250 m and temporal resolution with 16-day to analyze crop calendar according to Fig. 2. The algorithm used to generating the MOD13Q1 product chooses the best available pixel value from all the acquisitions from the 16-day period. The criteria used are low clouds, low view angle, and the highest NDVI value. Total number of 23 images was collected. First of all, the HDF format of the products was pre-processed by MODIS Conversion Toolkit (MCTK) in ENVI, then a stacked layer of NDVIs was prepared and used in agricultural croplands to figure out the phenology and growing season of each crop type. This step helps to decrease data redundancy of Landsat image collection. Accordingly, 23 MODIS NDVI time series grid data used to extract the phenology of different crop types (wheat and barley, rice, alfalfa, MC, and spring). It is essential to state that in this study Wheat and Barely considered in one class due to the great similarity of their spectral properties with each other. In addition, spring crops assign to crops growing in spring and harvesting in summer, similarly, MC crops assign to crops that are harvesting more than two times yearly. As shown in Fig. 2, the growing season of all crop types is divided into two main parts: first from DOY[1] 49 (18 of February) to late June, second from August to late November, while NDVIs in December and January had small fluctuation.

[1] Day of Year.

Landsat images

The use of Landsat series imagery in the study of land use and land covers has a very long history and has provided invaluable services for recognizing croplands and their types. The Operational Land Imager (OLI) on board Landsat-8 satellite, acquires data following a sun-synchronous orbit with a revisit interval of 16 days since 2013. OLI measures radiances in 11 spectral bands (in the range of 0.433–2.300 µm) covering the solar and the thermal domains. Instantaneous fields of view of the sensor correspond to a spatial resolution at the ground of 30 m for bands 1–9 (visible to middle infrared) and 100 m for bands 10 and 11 (thermal infrared band). Landsat images were obtained from the USGS website (http://glovis.usgs.gov).

According to Fig. 2, different crop types growing season happens between the ends of February to September. It indicates that Landsat images should be collected at least in 6 months (April, May, June, July, August, and September), the critical period in crop types growing seasons. In order to take the advantage of a similar spatial resolution of satellite images, a yearly temporal Landsat OLI cloud-free images assembled in 2016 including 14 images in the growing seasons. Landsat images radiometric correction (converting DN value to reflectance) were done via ENVI software, then a spectral subset of images produced by selecting 6 visible, infrared, and shortwave infrared bands. After all, a collection of spatial subsets of the study area was prepared for all images.

Field data

Ground truth data are an indispensable part of supervised classification as training and validation data. Each class gets its spectral and temporal properties based on training samples while validation samples are being used for accuracy assessment. Although, ground truth samples gathering is a sensitive deliberating task, these samples seriously affect classification results and accuracy. In this study, for each crop type, some samples were gathered during a pre-field observation in spring and fall of 2016. The number of polygons and percentage of training and validating samples of each class is presented in Table 3, and spatial distribution of the samples are shown in Fig. 1. Generally, about 42, 79, 25, 19, and 34 samples of wheat, rice, alpha, multiple-crop, and spring crop were collected, respectively, of which about 60% were used as training samples, and the remaining 40% were used as control samples.

Methodology

Pixel-based classification methods discriminate classes base on spectral attributes of each pixel and heterogeneity of adjacent pixels in cropland cause serious problems in croplands classification (Li et al. 2015). On the other hand, object-based image analysis (OBIA) classification using spatial context in addition to spectral attribute. Usage of OBIA has been increased recently to overcome the problem of pixel heterogeneity in an object (cropland) by merging homogenous spectral and textural objects (Blaschke 2010). In the present study, different crop types are classified with an OBIA classification with the combination of Rule based Decision Tree (RBDT) and OBNN (Object-based Nearest Neighborhood) in 3 main steps. First of all, homogenous croplands are extracted via a multiresolution segmentation using Landsat-OLI images. Secondary, ground observed samples introduced as a thematic layer to the model and the Nearest neighborhood classification has run to crop types definition using multi-temporal various vegetation Indexes (NDVI,[2] NDWI,[3] GNDVI[4]). Finally, other land covers, orchard, water lands, rangelands, and other fall croplands separated with a rule-based decision tree classification. The main steps of classification illustration are as follow:

Segmentation

The principle procedure in object-oriented classification and image interpretation is object delineation producing throughout the segmentation procedure (Li et al. 2008). In Land use and crop type studies by satellite images each agricultural field is assumed as an object and should be precisely extracted from satellite images. One of the reputed methods in homogenous area detection is multi-resolution segmentation that used frequently in different researches. This procedure is an optimum way in which a homogeneous segment comes from a given number of image objects minimizing the average heterogeneity and maximizing their homogeneity. It is mainly used in both extracting features that are characterized not purely by color but also by the shape of land use features from remote sensing imagery (Documentation 2011). Therefore, in this study, this method is used to extract land fields. The key factors in segmentation are segment size defining by scale parameter and homogeneity factor. Scale parameter (SP) controls the average image object size (Baatz 2000) by which bigger objects, merging more homogeneous areas, are being produced with a higher SP and vice versa. The homogeneity factor is the combination

[2] Normalized Difference Vegetation Index.

[3] Normalized Difference Water Index.

[4] Green Normalized Difference Vegetation Index.

of the proportion of shape and color in each segment. The color shows the role of input satellite image spectral values on a segment's homogeneity and shape represent how much smoothness and compactness a region is. A hierarchical network of image objects creates by different SPs, color, and shape proportion in segmentation (Darwish, Leukert, and Reinhardt 2003). In this research, several scale parameters (5, 2, 1, 0.8, 0.6) were tested to get so-called cropland using eCognition software. Since there are many small croplands low scales were examined with different input bands to get the appropriate size for croplands in the study area. Also, it should be considered that the quality of objects (geometrical parameters i.e. shape, extent) must be preserved in different scales. Quality assessment done to get suitable croplands objects throughout segmentation. though, visual interpretation (VI) is widely used for quality assessment of segmentation, Coasta declare that using a subjective VI result more suitable and acceptable outputs(Costa et al. 2018). Therefore, in this study, some parts of Landsat images containing many croplands selected to check out the quality of objects., then, the fitness of objects created with different SPs were visually interpreted. After setting the SP, different values of shape and color were tested. Since, the color factor is the main determinative factor using multi-spectral, medium resolution images (Landsat, Sentinel-2) it assumed that color gets higher amount while the shape factor gets minimum amounts. So the values of 0, 0.3 and 0.5 were test for shape and values of 0.9, 0.8… 0.3 were tested to color. The result objects of different color and shape factor fitness with the croplands on Landsat image were visually interpreted again. The results of the quality assessment showed the bests appropriate objects given on a scale of 0.8. After setting the scale parameter, shape, and color criterion were assessed. As in other researches denoted proper objects (cropland) are produced with a higher rate of color and low rates of shape (Pu and Landry 2012). Also, in this study color smoothness factor achieved the highest ratio of 0.9 while the shape ratio was zero. Although, the rates of SP (0.8), color (0.9), and shape (0) showed proper results for croplands delineation with using various combination of input bands of a single Landsat image, using the combination of Green, Red and NIR[5] bands have extracted the best boundaries for croplands.

Moreover, proper spectral band selection is a principle and delicate factor to object (each cropland) delineation especially using multi-temporal satellite images to cropland classification. Therefore, some consideration should be taken to get a segment fitting with the so-called cropland. In arid and semi-arid countries like Iran, in which rural inhabitant life is based on agriculture, farmers plant different crops in a land parcel. They regularly divide a land parcel into many sections were various kinds of crops sowing in different times of growing seasons. Fall crops, for example, have been sowing in fall and harvesting in spring. These kinds of sub-croplands are not detectable by using a single multispectral image. It is proven in different studies that Using two dates of images in growing seasons produces more accurate segments for classification than using a single date (Brooks et al. 2006).

In this study, it is proved that the best way of delineating a specific field with a special crop type is using spectral bands of two images in the growing period according to the crop calendar (one image in spring and the other in summer). Since spring cropland watered only based on wells, spring, and rivers and farmers cannot use rainwater to these lands. Farmers often divide some parts of rain-fed and fall croplands to spring and MC croplands. So, most of the spring croplands are a small part of other agricultural land except in developing agricultural lands. Also, spring crops are mostly highlighted in August and September and their vegetation indexes have their highest rate in these months. In contrast, fall crops like wheat and Barely are eminent in images of April and May. So, using the combination of two Landsat images (May and August) enhances all croplands. To come up to this end, spectral bands of these two images are used in the segmentation process to extract all kinds of croplands. However, different segments were extracted by using various combinations of images' bands, the best results were obtained with the combination of three bands of each image (green, red and infrared bands). So, these three bands of each image (total six bands of input images) weighted and other spectral bands get zero weight. Thereby, the combination of images in different months with various spectral band combinations was tested many times by changing input bands to get a suitable segmentation with the selected scale (i.e. 0.8, 0.6, and 1). The difference between segmentation via one image or using two images illustrated in Fig. 3. According to this figure, if segmentation is done using one image (image of May, with the highest crop density in the area) most of the small croplands with high crop density in August are not be extracted properly (Fig. 4 b and c). Meanwhile, incorporating the second image (image of August) the result changes totally and small fields will be discriminated. It is important that these croplands show how many times land is utilized for sowing different crops. Moreover, these small lands are allocating to a MC crop type or a single crop which are harvesting in spring or summer. Also, the results indicated that not only is the number of spectral bands significant in the shape of segmentation, but the month of the image also is effective. For example, most of the image objects using bands Green, Red, and NIR totally differ from the objects

[5] Near Infra-Red.

Fig. 3 Multi-resolution segmentation using temporal images (May and August) **a** the false-color image in May, **b** Applying Multi-resolution segmentation using spectral bands (green, red, and infrared) of one image (in May) **c** the same segmentation on August image, and **d** Applying Multi-resolution segmentation using spectral bands of two images (in May and August)

created using bands Red, NIR, and SWIR.[6] In this research, the best results were archived using the combination of bands of two images (images of May and August).

Classification

Besides investigating the main crops of the study area (wheat and barley, rice, alfalfa, MC, and spring), there are some orchards and fall crops ignored due to the lack of field data. If these classes are not removed from classification, they cause erroneous classes in cropland classification. Similarly, DT based on OBIA classification used to delineate main crop types (wheat and barley, rice, alfalfa, MC, and spring) and discriminate other land uses like orchards, dense fall croplands, and bare lands. Moreover, a common method to address these classes is using RBDT classification by using class hierarchy. So, RBDT classification is implemented by assigning thresholds to water lands, rangeland, bare lands, fall crops, and orchards to put aside from the main classification. Then, OBNN classification was assessed to classify crop types using samples thematic layer. The quality of results was statistically controlled to get the proper accuracy by computing overall accuracy, Kappa coefficient factor, product accuracy, and user accuracy. In OBNN classification, each object has a hierarchical relationship with its adjacent objects. Therefore, not only spectral information but also statistical and contextual information of objects are used to assign each object to an appropriate class. However, traditional pixel-based methods form based on spectral context. (Benz et al. 2004).

Vegetation indexes

Since different vegetation indexes are sensitive to crop type, sowing time, harvesting time, and growing seasons, a wide

[6] Short-Wave Infrared.

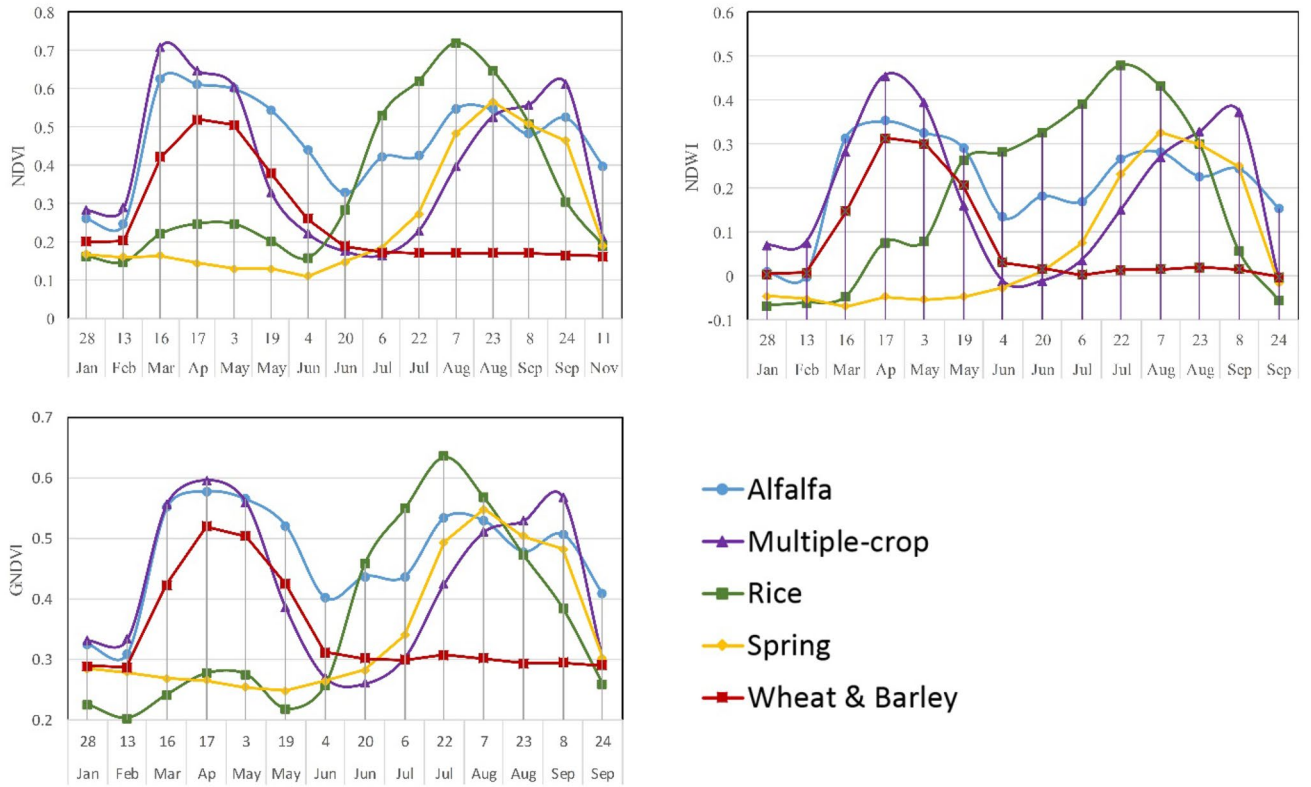

Fig. 4 Multi-temporal changes of different vegetation indexes for different crop types

range of vegetation indexes are being used in LULC change analysis and crop type monitoring by obviating the statistical analysis between spectral bands mainly in visible and near-infrared regions of the electromagnetic spectrum (Hoffmann and Blomberg 2004; Van Neil 2004). Vegetation indexes are analytically represented vegetation activity, vegetation biomass, and seasonal greenness changes. From different available indexes NDVI, EVI, GNDVI, and NDWI were tested to selected crop types and Landsat image bands. As the reaction of EVI was completely the same as NDVI it was put aside at the first steps. Other indexes were tested both individually and in combination for each crop type. The usage and definitions of different indexes that were used in the present study are as follow:

NDVI The most popular and privileged vegetation Index in LULC mapping and Crop type detection studies is the Normalized Difference Vegetation Index (NDVI) and has been used for analyzing the temporal and spatial variation of crops (Peña-Barragán et al. 2011; Wang 2014). Surveying of a single NDVI layer of an area in the growing season shows areas with a large amount of vegetation and areas with the lack of vegetation however, multi-temporal NDVI images shows biomass and greenery change of a crop type in the growing season (Jensen 2000; Yang 2003). NDVI is calculated by Eq. 1:

$$\mathrm{NDVI} = (\mathrm{NIR} - \mathrm{Red})/(\mathrm{NIR} + \mathrm{Red}) \quad (1)$$

GNDVI To reduce the effects of saturation, a number of additional indexes have been employed including the Green Normalized Difference Vegetation Index (GNDVI). This index is often used in UAV[7] images without the red band (Gitelson et al., 1996; Benvenuti and Weill, 2010). GNDVI is a simple index used for crop yield prediction in Burdikin (Robson et al. 2012). Equation 2, shows the relation of GNDVI and optical bands.

$$\mathrm{GNDVI} = (\mathrm{NIR} - \mathrm{Green})/(\mathrm{NIR} + \mathrm{Green}) \quad (2)$$

NDWI Normalized Difference Water Index is used widely to predict vegetation liquid water from space. As NDWI is calculated from NIR and SWIR (1.24 μm) bands, it is very sensitive to vegetation water and less sensitive to atmospheric effects than the NDVI index. Also, it is affected by

[7] Unmanned Aerial Vehicle.

vegetation canopy and growth especially for high vegetation coverage (e.g. alfalfa and rice) more than NDVI because of using reflectance SWIR band. Vegetation canopies in band 1.24 μm is a lot various than the red band's data (Gao 1996). Also, this index declines the early saturation factor causes in NDVI and it should be considered for vegetation coverage and crop yield (Huang et al. 2009). On the other hand, by accessing high spatial and temporal resolution, the multi-temporal of computed NDWI more likely to be taken into action. The NDWI is defined by Eq. 3.

$$\mathrm{NDWI} = (\mathrm{NIR} - \mathrm{SWIR})/(\mathrm{NIR} + \mathrm{SWIR}) \quad (3)$$

The effects of vegetation indexes in crop type classification are undeniable, adding or omitting one index changes overall accuracy, class separation, input bands priority for classification. Therefore, in this study, a crop type map was produced in five scenarios using different vegetation indexes (NDVI, NDWI, GNDVI) and their combination. DEM and slope map of the study area were the common layers in all scenarios, while vegetation indexes were variables. Three scenarios were conducted based on using multi-temporal images of NDVI, NDWI, and GNDVI lonely, then a combination of NDVI with NDWI performed as the fourth scenario, and finally the combination of NDVIs, NDWIs, and GNDVIs are used in the fifth scenario. Since the combination of GNDVIs with NDVIs and NDWIs had poor results they were omitted from the proposed scenarios.

Accuracy assessment

Many accuracy assessment methods have been examined in remotely sensing classification (Koukoulas and Blackburn, 2001). Confusion Matrix has been placed above all as a standard method for classification accuracy basis on which to both describe and characterize errors, leading to refurbish the classification results. The overall accuracy gives all classification accuracy, user and product accuracy say how much a particular class has been classified correctly (Foody 2002). In this study, confusion Matrix was performed with the ground through samples to validate classification in all five scenarios. The results of overall accuracy and Kappa coefficient of confusion matrix used for quality assessment of crop type classification. So, whenever the range of kappa coefficient and overall accuracy is high it means that results are predicted accurately with high quality.

Results and discussion

Crop calendar

Based on the obtained results (Fig. 2) in the first half of the growing season, most crops reach their first vegetation peak during the days 81–113, then in the second half reach their second peak between the days 225 and 273. The highlight points for rice have happened in day 145(24 of May). Although different crops' NDVI trends are separable, the trends of MC and Alfalfa are very similar to each other and the rates of time series of alfalfa are higher than MC crops. In contrast, the spring crop trend is the inversion of wheat and barley. The growing season of wheat and barley occurs in the first part, while the spring crop occurs in the second part and both crops in the other part have a plateau trend. Among all crop types, rice is the only crop type that can be easily discriminated from MODIS NDVI data, since its peak and turning points differs from other crops. In contrast, this figure helps to understand various crop phenology patterns.

Figure 2 illustrated that agricultural phenology patterns of investigating crops vary from February to November. Crops sawing and harvesting times are in February, June, September, and November, while their growing time is in April, May, and August. This figure also gives an outlook to select multi-temporal Landsat images (Medium resolution images) between day 49 (18 of February) to 321(16 of November).

Vegetation indexes description

A quick look at charts of different indexes extracted from multi-temporal Landsat images (Fig. 4) shows that in this area crops growing happens in two periods: first from February to June and the second from June to November (similar to MODIS NDVI). In contrast to MODIS NDVIs, there are separable trends between different crops. Each crop type reaches its apex in a definite time. For example, wheat and barley reach their highest rate at the first studying period whereas alpha has two apexes with some fluctuation in whole seasons. A detailed survey of each crop will clarify crop differences resulting in their precise extraction.

NDVI analysis

NDVI profiles analogy states NDVI rate in investigating crops alters from 0.1 in spring crops to 0.72 in rice crops. Also, it says NDVI rates of all crops at the beginning and end of the growing season are very close to each other and alter from0.14 to 0.28 except for alfalfa (at the end it is 0.39). Crops detail assessment indicates that wheat and barley crops growing season starts from late Feb and reaches its

maximum with a rate of more than 0.5 in April and then decrease to 0.18 in July and then after it remains stables. This trend is vice versa for spring crops, where the NDVI of these crops decreased very slowly from January to June, and then it goes up to 0.56 in August and after meeting MC crop in September decrease to 0.19 in November. Other crops, rice, alfalfa has two growing seasons, but the Rice trend is completely differing from MC and alfalfa. That means in the first part the maximum rate for Rice is 0.25 while it is more than 0.6 for MC and alfalfa. However, in the second growing part, Rice gets to its maximum rate of about 0.7 in the first half of August, whereas NDVI rates for MC and Alfalfa were between 0.52 and 0.62. Even though Alfalfa and MC crops trends are very similar, having two maximum points with some fluctuation, also, their trend in the second part of the growing season is more distinguishable than the first part., i.e., from June to late August MC crop lag behind the alfalfa, then go forward to its second surge point in late September around 0.65. The fluctuation of alfalfa is obvious in the second part. However, NDVIs turning point of Rice and spring crops are in the first half of June and others in late June and the main growing season of Rice and spring crops is in the second part. The NDVI rates of spring crops are less than Rice and it often lags behind the Rice especially in the second half except in September. It means spring crops biomass is less than Rice during a year. Finally, the NDVI images of studying crops are well-recognized and suitable for crop type detection.

GNDVI analysis

GNDVI profiles state both minimum and maximum rate of this index belong to Rice in February and July respectively and it was changed from 0.2 to 0.64. Also, GNDVIs rates of all crops except Rice at the beginning and end of the growing season are so similar. At the first growing season, the rates alter from 0.28 to 0.33 except in Rice and at the end of growing season, GNDVI rates change from 0.25 to 0.3 except for Alfalfa. Generally, GNDVI profiles state in the second half of growing seasons, the trends of all crops are extremely look like to NDVI. But, in the first part, they have some differences, NDVI profile of spring crops rate is lower than Rice, but according to GNDVI profile, Rice is behind the spring crop intersecting its chart in March and May.

Spring crops growing season starts from 4 of June intersecting both MC and Rice crops from 0.26 and rocketed up to 0.55 in August, then smoothly decreased to 0.48 in 8 of September and got to the lowest rate 0.31 in 24 of September in its harvesting time. Also, spring crops in the growing season showed some intersection with MC crops just before the peak point. Although, Rice crops have two peaks in April and July, the difference of them is about 0.36 which is than nine times greater than that of other peak crops naming MC and alfalfa (the difference of peak is around 0.04). In the first part of the growing season, Rice crops have two highlight points in 13 of February and 19 of May with a rate of around 0.2. This crop type escalated up from 19 of May to the 22 of July then fell steadily to reach 0.25 in September. Wheat and barley crops have one peek like NDVI in the first part and minimum and maximum GNDVI rates vary from 0.3 at the starting and ending point in January and September to 0.52 in April are in the middle place among other crops. Though the challenging products, MC and alfalfa, are not distinguishable in the first part and they have two intersections in the summit in March and 3 of May, their chart split off from May to the end of the studying period with a 0.1 lag. In the first part from May to the 7 of August, alfalfa crops had higher rates, and then after up to late September MC crop come to the top. While the up and down of alfalfa crops had little variation around 0.2, MC crop, difference between apogee and perigee is about 0.35.

Generally, the minimum and maximum rates of GNDVI belong to Rice, minimums happen in February, May and the maximum rate in July. MC crops have maximum lags with spring crops in the first part and with wheat and barley in the second part of growing seasons. The slope of MC crops trend in all indexes is the steepest before and after turning points.

NDWI trends

Evaluating of NDWI profile states that these profiles have significant difference with NDVI and GNDVI. Indeed, NDWI minimum rates for all crops were negative at the starting of the second part of the growing season. Also, NDWI rates alter between − 0.068 in spring crops and 0.48 in Rice crops. Comparing NDWIs profiles with other indexes indicates that trends of NDWI of various crops in the second part of growing seasons are more similar to NDVI trends, but in the first part similarity of NDWI, and NDVI and GNDVI series exist just in Wheat and barley and alfalfa. In addition, the NDWI trend of Rice entirely differs from other series. Although all crops have a turning point in June, Rice continues its climbing rate to get 0.48 in the second half of July. The main reason for this reaction of Rice crop is that its' growing inextricably depends on water which is distinguishable by NDWI. In comparison with NDVIs series, the maximum points for NDVI have happened in March (alfalfa, MC, spring), April (Rice, wheat and barley), August (MC, Rice), and September (spring and alfalfa), but the maximum points for NDWIs are in April in the first half of growing seasons and varies from July to September for Rice, spring and alfalfa and then for MC successively.

Rice NDWI trend goes upward from January to July reaches its highlight 0.5 on 22 of July and goes down steadily to 0.1 in September. Though NDVI trends of MC and

alfalfa are similar in the first part of growing seasons, their summit points get separated in the NDWI series. MC crops NDWI in the starting point of studying period is more than other crops and it gets to its first peak point in April, the fell to its turning point in 4 of June and surge up roughly to its second apex 0.4 in September, then fells down suddenly. However, trends of MC and wheat and barley are similar for NDWI indexes in the same period in which wheat and barley trend are coming behind MC, wheat, and barley crops after turning point leveled off to end of studying period. The trend of Alfalfa starts from zero in January goes up to 0.33 in April, then decrease to 0.15 in the turning point and then with some fluctuation goes up and down. Moreover, this trend in august reaches its second peak incident with spring crop and at the end of the studying period, its rate is 0.17 more than other crops final rate. The trend of the alfalfa crop states that it has a continuous growing season and its growth would happen several times in the year.

Also, MC crops reach their second apogee in September. Comparing the maximum rates priority of different crops indicates Rice and MC are prior then alfalfa. On the other hand, spring crops are in lower ranks and wheat and barley is the lowest according to NDVI and NDWI.

Crop type classification

The crop type maps of studying area in five proposed scenarios were produced interfering with different vegetation indexes using an OBIA classification method. In all scenarios used, rangelands, bare lands, small croplands, and water bodies are defined by decision tree classification. Then, five crop types were detected based on all scenarios using the nearest neighbor classification with input features optimization method. According to feature optimization and class distance matrix, the fifth scenario including all indexes was accepted as the best classification for these crop type extractions. Figure 5 shows the crop type map of studying area using multi-temporal NDVI, NDWI, and GNDVIs indexes and presents an output map of all scenarios in a small part of the study area where all crops variety and distribution is more than other parts.

The results of feature optimization and class separation distance matrix are given in Tables 1 and 3, respectively. According to Table 1, the best class separation distance has happened in scenarios 4 and 5 with the dimension of 19 and 21 successively. Remarkably, the Class separation distance matrix and each temporal index proportion in classification assessed during the classification process many times to get an acceptable result. Separation distance in the third scenario rating 0.14 was not acceptable at all, so the result of crop classification based on only GNDVI indexes produced poor results. In Contrast, the separation distance and dimension with using only NDVI or NDWI were very similar and In comparison with the separation distance of the fourth and fifth scenarios were not acceptable.

According to the class separation Matrix distance of the fifth scenario, class separation distances in most cases especially for Rice are more than 10, meaning that classes were separated correctly. This factor for MC and alfalfa has the minimum range comparing with other crops, i.e., 6.75. It means, MC and alfalfa crops may have been mixed with each other in some parts (Table 2).

In order to compare different scenario results, classification maps of a dense crop area with high crop variety are shown in Fig. 6. Referring to classification analysis by best separation distance and dimension of classification, it is clearly seen that maps of fourth and fifth scenarios are identical, whereas the maps of using only one Index completely differ from the others.

To have a better comparison of different scenarios each crop type's area in all scenarios is given in Table 3. According to Table 3, in all scenarios except scenario 2, the area of wheat and barley crop with the area around 550 km^2 is at the maximum, then alfalfa, MC, Rice, and spring crops are in the following rank respectively. As scenarios 1, 3, 4 and 5, the spring crops area is the least with the area of around 90 to 100 km^2. The area of wheat and barley crops are about five times as much as that of spring and Rice crops. Also, the area of alfalfa and MC is 4 times and 3 times as much as that of Rice crops, respectively. Same as the maps description, different crops area in scenarios 4 and 5 are inspiringly similar showing a difference about 100 km^2 lower in alfalfa and 100 km^2 more rate in wheat and barley crops in the third scenario (using NDWIs lonely). The difference between alfalfa and wheat and barley in the first scenario with the fifth scenario is more challengeable (the difference rate is about $\pm$ 200 km^2). The Orchard area in the three last scenarios is around 100 km^2 coming from decision tree classification. But, in scenario 2 Rice crops have the most area, then spring, wheat, and barley, alfalfa comes after and MC is the least which is totally different other scenarios.

Accuracy assessment has been done with computing confusion Matrix for all scenarios. Since the individual, product, and user accuracy of different scenarios were lower or similar to the fifth scenario, the confusion matrix of the fifth scenario is presented in this document to show the individual accuracy of each crop type. For other scenarios, it suffices to bring out the overall accuracy and kappa coefficient. Total accuracy assessment of the fifth scenario, using all vegetation indexes, is as Table 4 saying the overall accuracy and Kappa coefficient of crop type classification are 88% and 0.83, respectively, similar to other crop classification studies. Cropping patterns are classified in the Laurentian Great Lakes Basin using MODIS NDVI time with series with 84% (Lunetta, 2010).

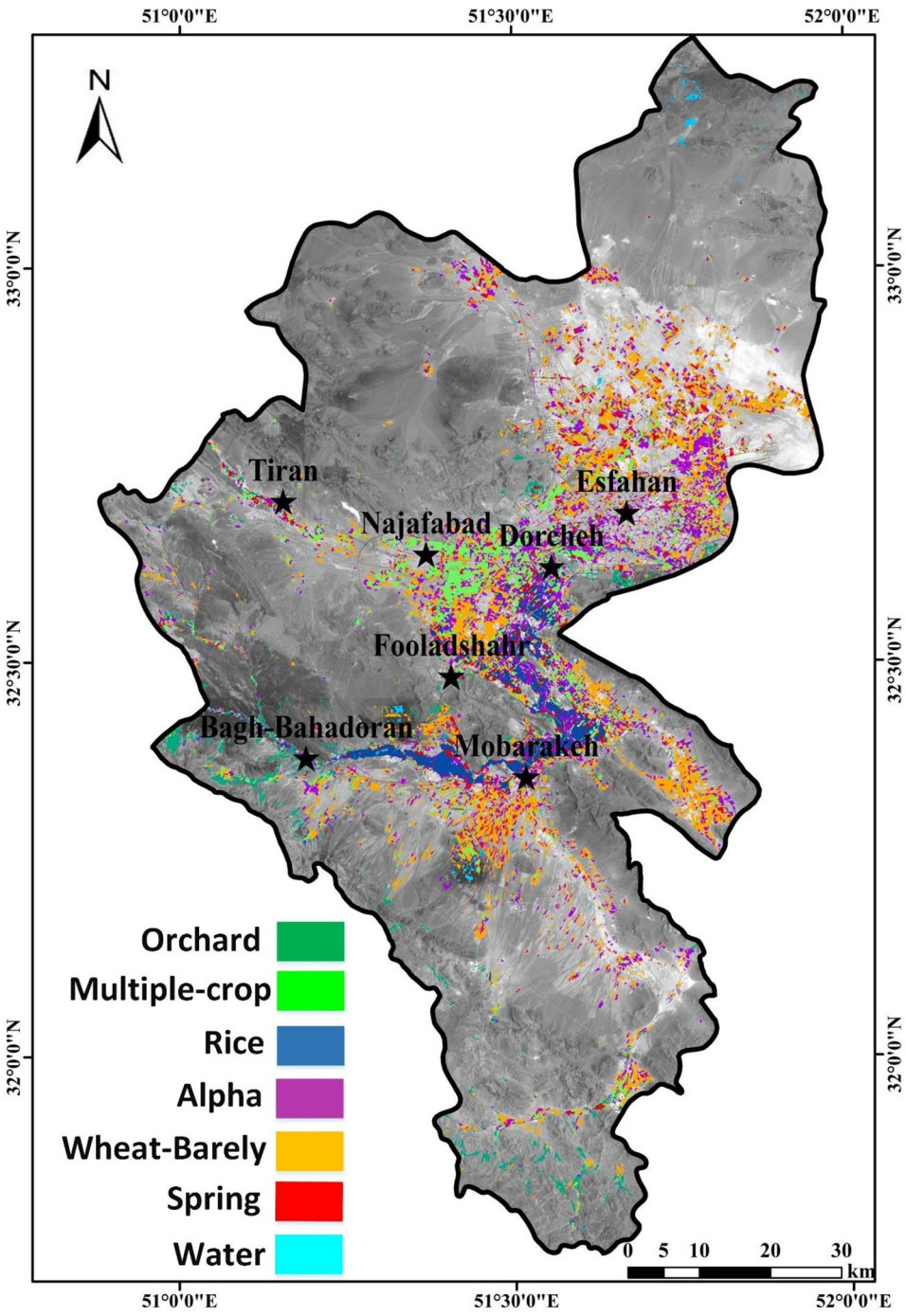

Fig. 5 Crop types map of the study area using a combination of NDVI, NDWI, and GNDVI

Crop type monitored using RapidEye time series with an overall accuracy of 87.46% (Kemal Sönmez et al. 2009). Object-based agricultural land classification with an enhanced time series of Landsat-MODIS images achieved 90.87% overall accuracy (Li et al. 2015). Table 4 also represents a detailed evaluating of individual crop types. It shows alfalfa crops mixed with MC resulted in a low rate of user accuracy. MC crops individual and product accuracy are lower than others simply because of their mixture with wheat and barley crops. Apart from MC crops, other crop types discriminated properly with an accuracy of more than 74%. On the other hand, the small size of MC fields embraces 2 or 3 Landsat pixels in comparison with other crop types in Isfahan nearby is another contributing

Table 1 Feature optimization results for different scenarios in object-based nearest neighbor classification

	Scenario 1 NDVI	Scenario 2 NDWI	Scenario 3 GNDVI	Scenario 4 NDVI + NDWI	Scenario 5 NDVI + NDWI + GNDVI
Best separation distance	4.62	4.26	0.14	6.63	6.75
Dimension	11	11	2	19	21

factor of its low accuracy. Alfalfa crops investigation shows that it has some combination with MC crops due to their similar NDVI and NDWI trends in the first part of the growing season. Also, it stats that spring crops have some mixture with Rice crops. The reasons for this combination are NDVIs similarity in rates of first part and trend in the first half of second growing season and their peek points in all indexes are very close to each other. In reality, spring crops life like Rice crops depends on irrigation during in second part of the growing season.

Other scenarios' overall and kappa coefficient factors have shown in Table 5. Comparing accuracy assessment of three first scenarios indicates that by using GNDVI merely the accuracy dramatically decreases to 34% which is not acceptable at all. On the contrary, the overall accuracy of using NDVI and NDWI separately are very similar to each other. Furthermore, using NDVI and NDWI simultaneously enhances the overall accuracy and kappa in the fourth and fifth scenarios.

Conclusion

In present study, crop type map of Isfahan and the nearby area produced with OBIA classification with the combination of RBDT and OBNN classifiers using Landsat-OLI temporal images and situ ground truth dataset in 2016. A series of common crop types including Wheat and Barley, Alfalfa, Rice, MC, and spring crops were selected for assessment. Time series of Landsat satellite images were collected according to crops phenology coming from MODIS NDVIs series. The processed satellite imagery datasets and ground truth data were input to OBIA classification which conducted includes OBNN and RBDT classifiers sequentially. The segmentation of proposed OBIA method conducted based on multi-resolution segmentation

Table 2 Class separation distance matrix in scenario 5

	Alpha	Dual	Rice	Wheat	Spring
Alpha	0	6.75	14.72	7.38	10.33
Multiple-crop	6.75	0	19.34	8.62	13.38
Rice	14.72	19.34	0	29.38	12.91
Wheat-barley	7.39	8.26	29.38	0	16.23
Spring	10.33	13.38	12.91	16.23	0

using multi-temporal Landsat images to extract croplands objects (segments). Using more than sole Landsat-OLI image implemented due to the crops complicated phonologies, implemented. At first, RBDT classification used to separate orchards, fall crops, Rain-fed farming lands, and non-agricultural lands in the study area. Then, OBNN classification is used for objective crop type classification. The OBNN classifier applied for different purposed scenarios using one or multi vegetation indexes to evaluate their performance to crop type discrimination. Nonetheless, the vegetation indexes play significant role in crop detection, their yearly trend asses in previous. Analogy of the time series of all vegetation index profiles implies some points: at first, there are two growing seasons in the studying area, at the second, MC and Alfalfa crops look to each other in the surging time. Thirdly, Rice, having the highest rate in all indexes, is the only crop that can be delineated using all indexes (NDVI, NDWI, or GNDVI). Fourthly, Wheat and Barley having one growing season with lower rates than other crops (i.e. MC, Alfalfa) remain stable in the second part of growing seasons. Fifthly, in the middle of the growing season from May to September Alfalfa shows a fluctuation trend. In order to achieve the right crops delineation, multi-temporal changes of three vegetation Indexes saying NDVI, GNDVI, and NDWI in 5 scenarios individually and with a combination of others (NDVI, GNDVI, NDWI, NDVI + NDWI, NDVI + NDWI + GNDVI) used with DEM and slope maps of studying area as input bands of OBNN classification. Object-based classification, distance matrix, and accuracy assessment of different scenarios state that using a combination of NDVI and NDWI gives a better result for selected crop types extraction. As the best separation distance and dimension of the fifth scenario with a combination of all indexes were the highest, it selected as an appropriate scenario. Furthermore, the accuracy assessments of all scenarios confirm using NDVI and NDWI combination simultaneously in fourth and fifth scenarios to extract objective crop types. Final crop map of studying area produced using all indexes with an overall accuracy of 88% and kappa 0.83. All crops extracted with high acceptable accuracy except MC in order to its mixture with Alfalfa crops. It should be consider that, the produced cropland map is belong to 2016 based on used images and a sample datasets. Accordingly, for future landscape, croplands classification, pattern detection and

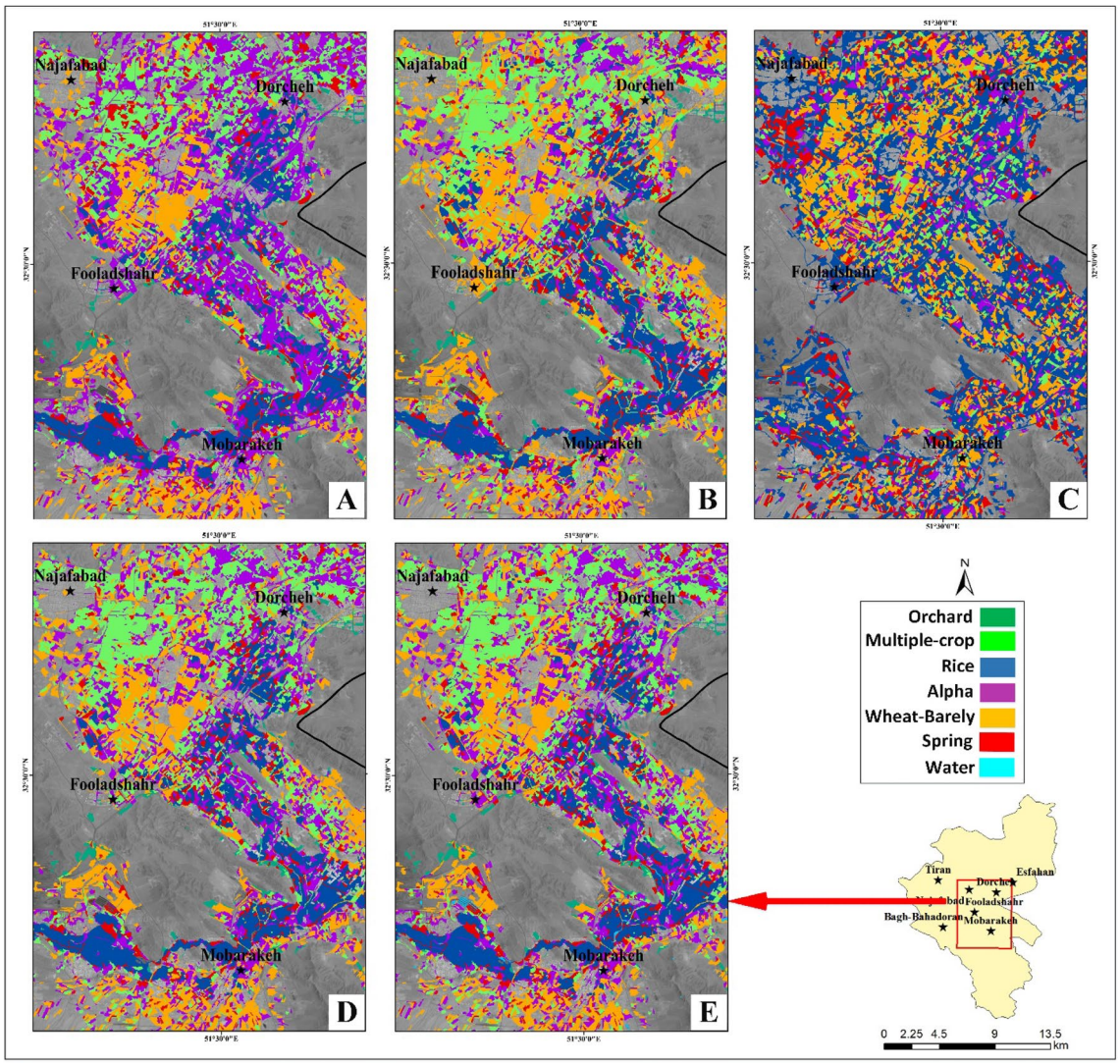

Fig. 6 Crop type classification maps in five scenarios with a different combination of vegetation indexes. **a** in scenario1 using only NDVI index, **b** scenario 2 using NDWI, **c** scenario 3 Using GNDVI, **d** Scenario 4 using both NDVI and NDWI, **e** scenario 5 using a combination of all Indexes (NDVI, NDWI, and GNDVI)

Table 3 Different crops areas in five named scenarios (Km^2)

	Scenario 5 NDVI + NDWI + GNDVI	Scenario 4 NDVI + NDWI	Scenario 3 NDWI	Scenario 2 GNDVI	Scenario 1 NDVI
Alpha	382.8	381.5	288.1	195.4	523.7
Multiple-Crop	272.8	277.5	268.5	113.4	224.7
Rice	105.3	103.5	130.9	1271	101.9
Spring	96.8	89.8	91.7	419	106.3
Wheat-barley	538.1	559.9	637.8	394.7	758.8
Orchard	97.88	120.5	93.8	57.7	370.1

development studies the spatial change of crop type in different years is essential. This study suggest to use three years or more multi-temporal multi-spectral images to separate fallow-lands, all major crop types and their spatial variation in different years.

Table 4 Error matrix for final object-based classification using all vegetation indexes

	Wheat	Spring	Rice	Multiple-crop	Alpha	User accuracy
Wheat	94.80	1.08	3.22	19.77	2.14	93.70
Spring	0.42	83.74	4.45	7.27	0.00	89.90
Rice	0	13.28	91.72	0.00	3.74	85.00
Multiple-crop	1.22	0.00	0.31	66.14	19.79	82.40
Alpha	3.55	1.90	0.31	6.82	74.33	55.20
product accuracy	94.8	83.74	91.70	66.10	74.30	
Overall accuracy = 88%						
Kappa coefficient = 0.83						

Table 5 Crop type detection accuracy using different vegetation indexes

	Scenario 1 NDVI	Scenario 2 NDWI	Scenario 3 GNDVI	Scenario 4 NDWI + NDVI	Scenario 5 NDVI + NDWI + GNDVI
Overall accuracy (%)	85.9	86.0	37.8	89.1	88.0
Kappa coefficient	0.79	0.79	0.18	0.83	0.83

Acknowledgements The authors acknowledge funding from the Water Research Institute (WRI) and Ministry of Energy for the ministration of datasets and for providing the computational and fieldwork facilities. The authors acknowledge teams' great cooperation and advices in Water Resource Department of Water Research Institute. We are very grateful to Esfahan Region Water Authority helping in crop sampling. We would also like to thank for Landsat and MODIS data that was freely available from USGS.

References

Alimudi S, SB Susilo, and JP Panjaitan (2017) Deteksi Perubahan Luasan Mangrove menggunakan Citra Landsat berdasarkan Metode Obia di Teluk Valentine Pulau Buano. Jurnal Teknologi Perikanan dan Kelautan 8(2): 139–146

Asgarian A, Soffianian A, Pourmanafi S (2016) Crop type mapping in a highly fragmented and heterogeneous agricultural landscape: a case of central Iran using multi-temporal Landsat 8 imagery. Comput Electron Agric 127:531–540

Baatz M (2000) Multiresolution Segmentation: An Optimization Approach for High Quality Multi-Scale Image Segmentation, Angewandte Geographische Informationsverarbeitung pp. 12–23

Belgiu M, Csillik O (2018) Sentinel-2 cropland mapping using pixel-based and object-based time-weighted dynamic time warping analysis. Remote Sens Environ 204:509–23. https://doi.org/10.1016/j.rse.2017.10.005

Benvenuti F, Weill M (2010) Relationship between multi-spectral data and sugarcane crop yield. In: Proceedings of the 19th World Congress of Soil Science and Soil Solutions for a Changing World pp. 33–36

Benz UC, Hofmann P, Willhauck G, Lingenfelder I, Heynen M (2004) Multi-resolution, object-oriented fuzzy analysis of remote sensing data for GIS-ready information. ISPRS J Photogramm Remote Sens 58(3-4):239–58. https://doi.org/10.1016/j.isprsjprs.2003.10.002

Blaschke, T (2010) Object Based Image Analysis for Remote Sensing. ISPRS J Photogramm Remote Sens 65:2–16. https://doi.org/10.1016/j.isprsjprs.2009.06.004

Brooks CN, Schaub DL, Powell RB, French NHF, Shuchman RA (2006) Multi-temporal and multi-platform agricultural land cover classification in southeastern Michigan. Ann Arbor 1001:48105

Castillejo-González IL, López-Granados F, García-Ferrer A, Peña-Barragán JM, Jurado-Expósito M, de la Orden MS, González-Audicana M (2009) Object-and pixel-based analysis for mapping crops and their agro-environmental associated measures using QuickBird imagery. Comput Electron Agric 68:207–15

Castro De, Ana I, Six J, Plant RE, Peña JM (2018) Mapping crop calendar events and phenology-related metrics at the parcel level by object-based image analysis (OBIA) of MODIS-NDVI time-series: a case study in central California. Remote Sens 10:1745

Chen S, Useya J, Mugiyo H (2020) Decision-level fusion of sentinel-1 SAR and Landsat 8 OLI texture features for crop discrimination and classification: case of Masvingo, Zimbabwe. Heliyon 6(11):e05358

Costa H, Foody GM, Boyd DS (2018) Supervised methods of image segmentation accuracy assessment in land cover mapping. Remote Sens Environ 205:338–351

Craig M. (2010) A history of the cropland data layer at NASS. USDA NASS CropScape

Darwish A, Leukert K, Reinhardt W (2003) Image segmentation for the purpose of object-based classification. In: International Geoscience and Remote Sensing Symposium 3:2039–2041

De Wit AJW, Clevers JGPW (2004) Efficiency and accuracy of per-field classification for operational crop mapping. Int J Remote Sens 25(20):4091–112

Do Bendini HN, Sanches ID, Körting TS, Fonseca LMG, Luiz AJB, Formaggio AR (2016) Using Landsat 8 image time series for crop mapping in a region of Cerrado, Brazil. Int Arch Photogramm Remote Sens Spat Inf Sci - ISPRS Arch 41:845–850. https://doi.org/10.5194/isprsarchives-XLI-B8-845-2016

Dongping Ming XZ, Wang M, Zhou W (2016) Cropland extraction based on OBIA and adaptive scale pre-estimation. Photogramm Eng Remote Sens 82:635–644

Fujihara Y, Tanakamaru H, Tada A, Adam BMA, Elamin KAE (2020) Analysis of cropping patterns in Sudan's Gash Spate Irrigation System using Landsat 8 images. J Arid Environ 173:104044

Ferrant S et al (2017) Detection of irrigated crops from sentinel-1 and sentinel-2 data to estimate seasonal groundwater use in South India. Remote Sensing 9(11):1119

Foody GM (2002) Status of land cover classification accuracy assessment. Remote Sens Environ 80:185–201

Fritz S, See L, McCallum I, Schill C, Obersteiner M, Van der Velde M, Boettcher H, Havlík P, Achard F (2011) Highlighting continued uncertainty in global land cover maps for the user community. Environ Res Lett 6:044005

Gao B-C (1996) NDWI—A normalized difference water index for remote sensing of vegetation liquid water from space. Remote Sens Environ 58:257–266

Gao F, Anderson MC, Zhang X, Yang Z, Alfieri JG, Kustas WP, Mueller R, Johnson DM, Prueger JH (2017) Toward mapping crop progress at field scales through fusion of Landsat and MODIS imagery. Remote Sens Environ 188:9–25

Georgi C, Spengler D, Itzerott S, Kleinschmit B (2018) Automatic delineation algorithm for site-specific management zones based on satellite remote sensing data. Precis Agric 19:684–707

Gerstmann H, Möller M, Gläßer C (2016) Optimization of spectral indices and long-term separability analysis for classification of cereal crops using multi-spectral RapidEye imagery. Int J Appl Earth Obs Geoinf 52:115–125

Gerstmann H et al (2018) Detection of phenology-defined data acquisition time frames for crop type mapping. PFG J Photogram Remote Sens Geoinf Sci 86(1):15–27

Gitelson AA, Kaufman YJ, Merzlyak MN (1996) Use of a green channel in remote sensing of global vegetation from EOS-MODIS. Remote Sens Environ 58:289–98. https://doi.org/10.1016/S0034-4257(96)00072-7

Hilker T, Wulder M, Coops NC, Linke J, McDermid G, Masek JG, F. o, and J.C White. (2009) 'A new data fusion model for high spatial- and temporal-resolution mapping of forest disturbance based on Landsat and MODIS. Remote Sens Environ 113:1613–1627

Hoffmann CM, Blomberg M (2004) Estimation of leaf area index of Beta Vulgaris L. based on optical remote sensing data. J Agron Crop Sci 190:197–204

Huang H, Legarsky J, Othman M (2007) Land-cover classification using Radarsat and Landsat Imagery for St.Louis, Missouri. Photogramm Eng Remote Sens 73:37–43

Huang J, Chen D, Cosh MH (2009) Sub-pixel reflectance unmixing in estimating vegetation water content and dry biomass of corn and soybeans cropland using normalized difference water index (NDWI) from satellites. Int J Remote Sens 30:2075–2104

Immitzer M, Vuolo F, Atzberger C (2016) First experience with Sentinel-2 data for crop and tree species classifications in central Europe. Remote Sens 8:166

Jensen, J.R. (2000) An earth resource perspective, Upper Saddle River, New Jersey. Remote sensing of the environment

Kemal Sönmez N, Onur I, Sari M, Maktav D (2009) 'Monitoring changes in land cover/use by CORINE methodology using aerial photographs and IKONOS satellite images: a case study for Kemer, Antalya, Turkey. Int J Remote Sens 30:1771–1778

Khan MS et al (2020) An artificial neural network model for estimating Mentha crop biomass yield using Landsat 8 OLI. Precis Agric 21(1):18–33

Koukoulas S, Blackburn GA (2001) Introducing new indices for accuracy evaluation of classified images representing semi-natural woodland environments. Photogramm Eng Remote Sens 67(4):499–510

Kussul N, Lemoine G, Gallego FJ, Skakun SV, Lavreniuk M, Shelestov AY (2016) Parcel-based crop classification in Ukraine using Landsat-8 data and Sentinel-1A data. IEEE J Select Top Appl Earth Observ Remote Sens 9:2500–2508

Kussul N et al (2017) Deep learning classification of land cover and crop types using remote sensing data. IEEE Geosci Remote Sens Lett 14(5):778–782

Lebourgeois V et al (2017) A combined random forest and OBIA classification scheme for mapping smallholder agriculture at different nomenclature levels using multisource data (simulated Sentinel-2 time series, VHRS and DEM). Remote Sens 9(3):259

Li HT, Gu HY, Han YS, Yang JH (2008) An efficient multi-scale segmentation for high-resolution remote sensing imagery based on statistical region merging and minimum heterogeneity rule (Vol 4)

Li Q, Wang C, Zhang B, Linlin Lu (2015) Object-based crop classification with Landsat-MODIS enhanced time-series data. Remote Sensing 7:16091–16107

Lunetta RS, Shao Y, Ediriwickrema J, Lyon JG (2010) Monitoring agricultural cropping patterns across the Laurentian Great Lakes Basin using MODIS-NDVI data. Int J Appl Earth Obs Geoinf 12(2):81–8. https://doi.org/10.1016/j.jag.2009.11.005

Manakos I, and S Lavender (2014) Remote sensing in support of the geo-information in Europe. In, Land use and land cover mapping in Europe (Springer)

Molle F, and P Wester (2009) River basin trajectories: societies, environments and development (IWMI)

Pani P, Jia L, Menenti M, Hu G, Zheng C, Chen Q, Zeng Y (2020) Evaluating crop water requirements and actual crop water use with center pivot irrigation system in Inner Mongolia of China. EGU General Assembly Conference Abstracts

Peña-Barragán JM, Ngugi MK, Plant RE, Six J (2011) Object-based crop identification using multiple vegetation indices, textural features and crop phenology. Remote Sens Environ 115:1301–1316

Pu R, Landry S (2012) A comparative analysis of high spatial resolution IKONOS and WorldView-2 imagery for mapping urban tree species. Remote Sens Environ 124:516–533. https://doi.org/10.1016/j.rse.2012.06.011

Robson A, C Abbott, D Lamb, and R Bramley (2012) Developing sugar cane yield prediction algorithms from satellite imagery. In: conference of the Australian society of sugar cane technologists

Schreier J, Ghazaryan G, Dubovyk O (2020) Crop-specific phenomapping by fusing Landsat and Sentinel data with MODIS time series. Eur J Remote Sens 54:47–58

Sencan, S. (2004) Decision tree classification of multi temporal images for field based crop mapping, school of natural and applied science

Thenkabail PS, Biradar CM, Noojipady P, Dheeravath V, Li Y, Velpuri M, Gumma M, Obi Reddy P, Gangalakunta HT, Cai X (2009) Global irrigated area map (GIAM), derived from remote sensing, for the end of the last millennium. Int J Remote Sens 30:3679–3733

Torbick N et al (2017) Monitoring rice agriculture across myanmar using time series Sentinel-1 assisted by Landsat-8 and PALSAR-2. Remote Sens 9(2):119

Ulaby FT, Moore RK, Fung AK (1982) Microwave remote sensing active and passive from theory to applications. Artech House: Massachusetts, Vol 3, pp. 1115-20

Van Neil TG, Mc Vicar TR (2004) Determining temporal windows for crop discrimination with remote sensing, a case study in south-eastern Australia. Comput Electron Agric 45(1–3):91–108

Vancutsem C, Marinho E, Kayitakire F, See L, Fritz S (2012) Harmonizing and combining existing land cover/land use datasets for cropland area monitoring at the African continental scale. Remote Sens 5:19–41

Vieira MA, Formaggio AR, Rennó CD, Atzberger C, Aguiar DA, Mello MP (2012) Object based image analysis and data mining applied to a remotely sensed Landsat time-series to map sugarcane over large areas. Remote Sens Environ 123:553–562

Vizzari M, Santaga F, Benincasa P (2019) Sentinel 2-based nitrogen VRT fertilization in wheat: comparison between traditional and simple precision practices. Agronomy 9:278

Wang C, Zhong C, Yang ZJ (2014a) Assessing bioenergy-driven agricultural land use change and biomass quantities in the U.S. Midwest with MODIS time series. Appl Remote Sens 8:1–16

Wang C, Zhong C, Yang Z (2014b) Assessing bioenergy-driven agricultural land use change and biomass quantities in the US Midwest with MODIS time series. J Appl Remote Sens 8:085198

Weigand M, Staab J, Wurm M, Taubenböck H (2020) Spatial and semantic effects of LUCAS samples on fully automated land use/land cover classification in high-resolution Sentinel-2 data. Int J Appl Earth Obs Geoinf 88:102065. https://doi.org/10.1016/j.jag.2020.102065

Yang C-C, Prasher SO, Goel PK (2003) Differentiation of crop and weeds by decision-tree analysis of multi-spectral data. Trans Am Soc Agric Eng 47(3):873–879

Zaki NAM, et al. (2020) Dominant tree species estimation for tropical forest using pixel-based classification support vector machine (SVM) and object-based classification (OBIA). In: Charting the sustainable future of ASEAN in science and technology. Springer: Singapore pp. 319–333